HEALTH MONITORING OF HELICOPTER DRIVE TRAIN COMPONENTS BASED ON SUPPORT VECTOR DATA DESCRIPTION

V. Camerini[a,b], G. Coppotelli[a], and S. Bendisch[b]

[a] *Department of Mechanical and Aerospace Engineering, University of Rome "La Sapienza", 00184 Rome, Italy*
[b] *Airbus Helicopters Germany, 86609 Donauwörth, Germany*

Abstract

The objective of the paper is to develop a vibration-based automated procedure dealing with early detection of mechanical degradation of helicopter drive train components using Health and Usage Monitoring Systems (HUMS) data. An anomaly-detection method devoted to the quantification of the degree of deviation of the mechanical state of a component from its nominal condition is developed. Such a method introduces an Anomaly Score (AS) as the combination of a set of statistical features correlated with specific damages, also known as Condition Indicators (CIs), thus implicitly including the operational variability in the model through the CI correlation. The problem of fault detection is thus recast as a one-class classification problem in the space spanned by a set of CI, with the aim of a global differentiation between normal (healthy) and anomalous (faulty) observations. In this paper, a procedure based on an efficient one-class classification method, not requiring any assumption on the data distribution, is used. The core of such an approach is the Support Vector Data Description (SVDD), that allows for obtaining good data descriptions without the need of a significant amount of statistical data. Several analyses are carried out in order to validate the proposed procedure, using flight vibration data collected from a H 135 (formerly known as EC 135) servicing helicopter, for which micro-pitting damage on a gear was detected by HUMS and assessed through visual inspection. The capability of the proposed approach of providing better trade-off between false alarms rate and missed detection rates with respect to individual CI and to the ASs obtained assuming Gaussian-distributed CI has been analysed.

1. INTRODUCTION

The problem of early fault detection is crucial in helicopter maintenance strategy. Early stage, undetected damage affecting critical sub-systems can progressively increase causing the system to fail. In the best case, such a scenario could result in increased operating costs for the machine owing to the required grounding time, maintenance and part replacement, as well as it could lead to dangerous accidents in some cases. The drive train sub-system is responsible for transferring power from the engines to the rotors, and represents a critical sub-system for the machine due to non-redundant load paths and the high variability of the dynamic loads acting on the components ([1]). As to ensure aircraft airworthiness, the system needs to be maintained following a prescribed preventive maintenance program, resulting in a burden to operating costs and aircraft availability. Therefore, Health and Usage Monitoring Systems (HUMS), defined as equipment/techniques/procedures by which selected incipient failure or degradation can be determined in [2], were introduced in the last decades in helicopter industry as a mean of increasing safety and reducing maintenance costs by enabling Condition Based Maintenance (CBM) ([3, 4]). Because damages are not directly observable, it is necessary to measure quantities which are affected by fault development. Mechanical degradation affects the vibration signature emitted from drive train rotating components. Moreover, technologies for measuring vibration signals are readily available. Therefore, it is common in the helicopter industry to equip rotating parts in the drive train with sensitive sensors (typically accelerometers) able of recording dynamic oscillation. The HUMS includes a transmission monitoring function which uses three types of data ([5]): accelerometer and tachometer signals, as well as contextual parameters such as airspeed, temperature and engine torque. Accelerometers are typically mounted on gearboxes and shaft bearings, tachometers on rotor shafts. The contextual parameters, when available, usually come from sensors which are part of other avionic/navigation systems than HUMS. Within the HUMS, a diagnosis logic

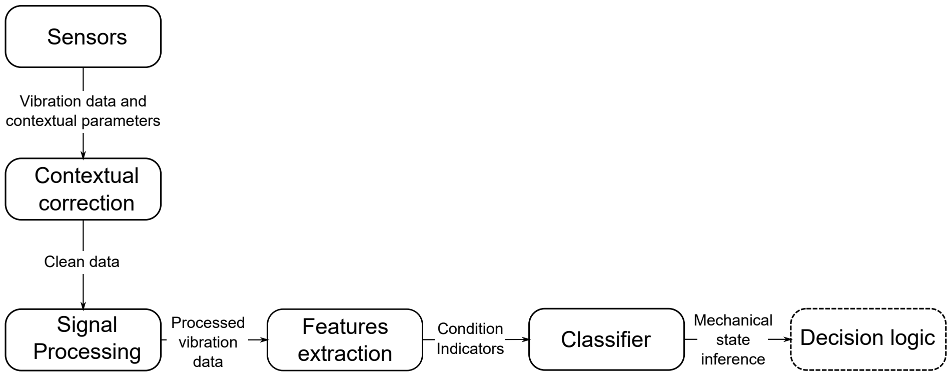

Figure 1: High level overview of HUMS diagnosis process.

is implemented in order to process a set of sensor signals by which the mechanical state of underlying assets is inferred. Figure 1 represents an overview of the diagnosis process. Sensor data are in a first step corrected for the contextual parameters. Invalid data, like noisy acquisitions or data recorded in unfavourable conditions (e.g. during run-ups or other non-stationary conditions of the machine) are rejected at this stage (contextual correction in figure 1. Features extraction consists of converting the raw sensor input in a metrics which is more informative about the state of the system ([6]), such features are commonly referred to as Condition Indicators (CI). Finally, CI are interpreted as an input to a classifier, with the aim of producing the most likely decision about the state of the monitored components. The inference may be as simple as deciding if a fault is present (fault detection), up to providing prognostic information on the remaining useful life for a given component. Such information is then passed to the overlying decision logic, supporting the maintenance decision process. Traditional HUMS ([7]) are based on univariate monitoring of each CI. The values of each CI are compared to an individual threshold, computed from fleet historical data. An alert is generated whenever any of the CI exceeds its threshold. However, the high variability of aerodynamic loads, transmission loads and operating conditions affect the vibration signature, resulting in high scattering of the CI values ([8, 9]). Therefore, despite the efforts in developing damage-sensitive features using advanced signal processing techniques, state-of-the-art HUMS are prone to increased false alarms ([10]). A novel approach to the CI analysis was developed in a five-year research program involving GE aviation ([10]), where multiple CI from fleet data are combined in a single Anomaly Score (AS). Such an AS represents the degree of deviation of an acquisition from the nominal state, defined using a Gaussian Mixture Models (GMM) based on the entire fleet multivariate data as a reference. Results revealed that this feature-level data fusion was capable of enhancing fault detection performance of classical HUMS analysis methods, neither requiring restrictions on operating conditions nor explicit modelling of their effects on the CI values. Contemporary, the research at Airbus Helicopters (AH) resulted in a different strategy, adopted in [11], where CI are combined in a so-called Health Indicator (HI) using the definition of Mahalanobis Distance. The HI are defined based on a set of CI for each component, and the nominal state definition relies on few acquisitions following a maintenance action. Differently from [10], this method aims to model a baseline for each individual component, independently from fleet data, thus preventing the between-helicopters variability due to different configurations and installation tolerances ([12]) to mask local trends in the CI. However, an intrinsic limitation of the methodology is in the obvious impossibility of detecting manufacturing defects. Besides, Gaussian assumption of the CI distribution is required. Actually, the fault detection problem can be considered as a one-class classification problem, with the task of separating the normal (healthy) data samples from the faulty ones. Support Vector Description (SVDD) is an unsupervised machine learning method specifically developed for solving the one-class classification problem by Tax and Duin ([13]). SVDD solves the problem of data description given a set of training samples, from which the boundaries of the target distribution are learnt. This approach has been successfully employed in image classification problems, one-class pattern recognition, damage detection, batch process monitoring, etc. (e.g. [14–17]). Examples of the application of SVDD in machine condition monitoring are found in [18–21]. In this paper, fault detection using HUMS data is recast as an anomaly detection problem in the space spanned by multiple CI as in [10]. In order to account for between-helicopters variability in the same fleet, individual component models are proposed as in [11]. The operational variability is implicitly accounted for in the model through the correlation induced within CI. Furthermore, since CI were preliminarily observed to be non-linearly correlated, with non-normal marginal distributions, a SVDD model is used for data description. The SVDD output is used as an AS, quantifying the degree of abnormality of an observation from the nominal distribution. The remainder of this paper is organised as follows. First, a theoretical background is given in Section 2. Extraction of CI from vibration data is introduced, then the basic SVDD model is presented and the proposed methodology described. In Section 3, the proposed methodology is evaluated on vibration data from a servicing H 135 (formerly known as EC 135) with a developing micro-pitting damage. Such data are collected in real operating conditions, extracted CI present therefore the associated scattering. It is shown that the developed algorithm can be applied in an operational framework, producing an AS which increases the separation between normal and faulty data with respect to individual CI and to a multivariate model based on Gaussian assumption. Finally, conclusions are made in Section 4.

2. THEORETICAL BACKGROUND

2.1. Extraction of Condition Indicators from vibration data

The general problem of CI extraction from accelerometers response in complex machinery is briefly introduced using a linear model, then, considering the specific case of gear pitting, the procedure adopted for defining related CI is described. Among the many techniques proposed in literature for gear local fault detection (see, e.g. [22–27], statistical features extraction based on the so-called synchronous average signal is considered in this work for its simplicity and proved effectiveness. Moreover, the limited sampling frequency of available sensors represents a constraint to the application of more advanced techniques like the ones based on the Spectral Kurtosis (SK) filtering procedure developed by Antoni et al. ([28, 29]), aimed to exploit system resonant bands as to amplify the early stage, impulsive fault signature.

2.1.1 Model of accelerometer response

The vibration response of the structural components to the operational excitation is assumed to be linear in the considered frequency range. The linear model for the response x_j at position j in a mechanical environment characterised by multiple vibration sources is then given as ([30]):

$$
\begin{aligned}
x_j(t,\theta) = &\sum_{i=1}^{NF} h_{ij}^F(t,\theta) * F_i(t,\theta)+ \\
&+\sum_{i=1}^{NI} h_{ij}^I(t,\theta) * I_i(t,\theta)+ \\
&+h_j^S(t,\theta) * m(t,\theta) + n_j(t,\theta),
\end{aligned}
\tag{1}
$$

where $*$ denotes the convolution operation, t and θ respectively the short time-scale associated with measurements and the long time-scale characteristic of the monitoring process. In the following, the dependency of the vibration signal over θ is dropped from the notation. The response is then given as the sum of NF fault-related signals $F_i(t)$ and NI interfering machinery signals $I_i(t)$ respectively convolved with the impulse response functions $h_{ij}^F(t)$ and $h_{ij}^I(t)$. The term $h_j^S(t) * m(t)$ explicitly introduces in the model the modal response at location j due to all remaining excitation sources from normal machine operation and imperfections. Finally, $n_j(t)$ models the ambient and sensor noise. From equation (1), the measured acceleration at the transducer location is the convolutive mixture of multiple sources. The identification of fault-related signatures requires isolating them from the rest of the signal, filtering out those interfering components related to the functioning of the healthy state machinery in its actual operating environment. Therefore, an understanding of the properties of fault or normal vibration is mandatory ([31]). Besides, the model of equation (1) includes the dependency of the measured vibration on the mode shapes of the system (and consequently the sensor position as well), the operating state of the machine and the transmission paths from the sources to the accelerometer.

2.1.2 Condition Indicators extraction based on the shaft-synchronous signal

The gear motion error signal, according to [32] can be defined as the difference between the gear's real motion and the ideal uniform motion. For a pair of meshing gears running at constant speed, the single gear motion signal can be deduced by ideal tangential displacement $x_i(t)$ at the pitch circle:

$$x_i(t) = x_0 + v_0 t, \tag{2}$$

with x_0 and v_0 initial displacement at the reference time t equal to zero and constant pitch line velocity. Considering the motion error, equation (2) becomes:

$$x(t) = x_0 + v_0 t + x_{eg}(t) + x_{es}(t), \tag{3}$$

where x_{eg} and x_{es} are given as infinite cosine series with fundamental period equal respectively to the gear mesh frequency f_g and the shaft frequency f_s:

$$x_{eg}(t) = \sum_{k=0}^{\infty} A_k cos(2\pi k f_g t + \alpha_k) \tag{4}$$

$$x_{es}(t) = \sum_{k=0, k\neq Z}^{\infty} B_k cos(2\pi k f_s t + \beta_k). \tag{5}$$

The coefficients A_k,B_k,α_k,β_k in equations (4) and (5) are amplitudes and phases of the k-th harmonic, whereas Z is the number of teeth of the considered gear (recall that the gear mesh frequency f_g is defined as the product of Z by the shaft rotating frequency f_s). Taking the second time-derivative of equation (3) gives the expression for the gear motion error acceleration signal:

$$\begin{aligned} a(t) = &- \sum_{k=0}^{\infty} (2\pi k f_g)^2 A_k cos(2\pi k f_g t + \alpha_k) \\ &- \sum_{k=0, k\neq Z}^{\infty} (2\pi k f_s)^2 B_k cos(2\pi k f_s t + \beta_k). \end{aligned} \tag{6}$$

Under the assumption of linear behaviour of the accelerometer response model (section 2.1.1), the measured acceleration signal contains the same harmonics of equation (6). Hence, a common technique for isolating the vibration signature related to a specific gear, the time-domain synchronous averaging (TSA) ([33, 34]) is used to identify such harmonic components.In order to prevent from jittering effects due to speed fluctuations in normal operating conditions, the measured signal is resampled to the angular domain before averaging (some authors refer to the TSA in angular domain as angular-domain synchronous averaging, see e.g. [23]). Speed fluctuations are implicitly assumed as small as not to provoke significant changes in the transfer functions of the system. After the extraction of the shaft-synchronous signal, the following CI are considered for fault detection:

1. Root Mean Square energy of the discrete signal (RMS)

   $$RMS = \frac{1}{N_s - 1} \sum_{k=1}^{N_s} (x_{TSA}(k\Delta\phi)) - \bar{x}_{TSA})^2 \tag{7}$$

   where k indicates the sample number, $\Delta\phi$ the samples spacing in the angular domain, N_s the number of samples and $\bar{x}_{TSA}$ the mean value of the shaft-synchronous signal samples. The RMS, or variance of the signal, is a measure of the overall energy level of the signal. It is therefore expected to increase due to the energy associated with local impacts caused by local faults in the gear.

2. Kurtosis of the signal (KRT)

   $$KRT = \frac{\sum_{k=1}^{N_s} (x_{TSA}(k\Delta\phi) - \bar{x}_{TSA})^4}{(Ns-1)RMS^2}, \tag{8}$$

   The kurtosis of a signal is the scaled fourth statistical moment and increases with increased signal impulsiveness. The kurtosis is expected to increase due to the fault, since the impacts from the pitted teeth are of impulsive nature.

Considering such indicators provides a set of two CI deemed able of separating the pitted gear vibration from the normal gear vibration. However, if different failure modes are taken into account, more indicators can be considered ([35]). Nevertheless, considering a set of indicators able of reacting to the fault is sufficient for the purpose of this work.

2.2. Support Vector Data Description

SVDD is a data domain description method inspired by the support vector machines ([36–38]). The basic idea is to determine, from a small set of training samples, the minimal volume hypersphere enclosing most of the target data. New instances outside the boundaries of the describing hypersphere are then classified as outliers. SVDD is suitable for the problem of fault detection when fault data are not available, since it only requires normal (target) objects in order to find a description of the normal state. The problem can be cast as a standard quadratic optimization with unique optimal solution ([39]), resulting in high computational efficiency for the method. In the following, the SVDD method is briefly introduced. One can refer to [13] for theoretical details. Assume a training set composed of M objects $\{\mathbf{x}_i, i = 1, 2, ..., M\}$ which are drawn from the target distribution. Being $\mathbf{a}$ the center of the hypersphere and R its radius, the cost function to be minimised reads:

$$F(R, \mathbf{a}) = R^2, \tag{9}$$

subject to the constraints:

$$||\mathbf{x}_i - \mathbf{a}||^2 \leq R^2, \qquad \forall i. \tag{10}$$

Cost function (9) is modified as to allow the possibility to reject some training points from the description, introducing slack variables $\xi_i \geq 0$ such that large distances from the center $\mathbf{a}$ are penalised:

$$F(R, \mathbf{a}) = R^2 + C \sum_i \xi_i. \tag{11}$$

Constraints (10) hence become:

$$||\mathbf{x}_i - \mathbf{a}||^2 \leq R^2 + \xi_i, \qquad \xi_i \geq 0, \qquad \forall i. \tag{12}$$

The parameter C controls here the trade-off between the volume of the hypersphere and the errors. Incorporating the constraints (12) into equation (11) by using Lagrange multipliers $\alpha_i \geq 0$ and $\gamma_i \geq 0$ leads to:

$$\begin{aligned} L(R, \mathbf{a}, \alpha_i, \gamma_i, \xi_i) = \\ &= R^2 + C \sum_i \xi_i - \sum_i \alpha_i \{R^2 + \\ &+ \xi_i - [\|\mathbf{x_i}\|^2 - 2(\mathbf{a} \cdot \mathbf{x}_i) + \\ &+ \|\mathbf{a}\|^2]\} - \sum_i \gamma_i \xi_i. \end{aligned} \tag{13}$$

In (13), L should be minimised with respect to $R, \mathbf{a}, \xi_i$ and maximised with respect to the Lagrange multipliers α_i and γ_i. Setting to zero the partial derivatives gives the constraints:

$$\frac{\partial L}{\partial R} = 0 : \qquad \sum_i \alpha_i = 1 \tag{14}$$

$$\frac{\partial L}{\partial \mathbf{a}} = 0 : \qquad \mathbf{a} = \sum_i \alpha_i \mathbf{x}_i \tag{15}$$

$$\frac{\partial L}{\partial \xi_i} = 0 : \qquad C - \alpha_i - \gamma_i = 0. \tag{16}$$

From (16) and from the Lagrange multipliers being non-negative, the γ_i can be removed by imposing:

$$0 \leq \alpha_i \leq C. \tag{17}$$

Substituting back (14)–(16) into (13) results in:

$$L = \sum_i \alpha_i (\mathbf{x}_i \cdot \mathbf{x}_i) - \sum_{i,j} \alpha_i \alpha_j (\mathbf{x}_i \cdot \mathbf{x}_j), \tag{18}$$

subject to the constraints (17). Now when a training object $\mathbf{x}_i$ strictly satisfies the inequality in (12), the constraint is satisfied and the corresponding α_i is zero. Differently, when (12) holds with equality, the constraint has to be enforced ($\alpha_i > 0$). Hence:

$$||\mathbf{x}_i - \mathbf{a}||^2 < R^2 \rightarrow \alpha_i = 0, \gamma_i = 0 \tag{19}$$

$$||\mathbf{x}_i - \mathbf{a}||^2 = R^2 \rightarrow 0 < \alpha_i < C, \gamma_i = 0 \tag{20}$$

$$||\mathbf{x}_i - \mathbf{a}||^2 > R^2 \rightarrow \alpha_i = C, \gamma_i > 0. \tag{21}$$

Since from equation (15), the center of the sphere is a linear combination of the objects, only training objects for which $\alpha_i > 0$ are needed for the description and they are therefore named support vectors (SV's) of the description. Besides, SV's lie on the boundary of the hypersphere, hence R^2 can be obtained as the distance from any SV to the center of the hypersphere $\mathbf{a}$. The distance of any new object $\mathbf{z}$ from the center of the hypersphere is then computed as:

$$\begin{aligned} \Delta(\mathbf{z}) = \|\mathbf{z} - \mathbf{a}\|^2 = \\ &= (\mathbf{z} \cdot \mathbf{z}) - 2 \sum_i \alpha_i (\mathbf{z} \cdot \mathbf{x}_i) + \\ &+ \sum_{i,j} \alpha_i \alpha_j (\mathbf{x}_i \cdot \mathbf{x}_j). \end{aligned} \tag{22}$$

In order to allow for more flexible boundaries (i.e. when data do not follow a spherical distribution), the inner product $(\mathbf{x}_i \cdot \mathbf{x}_j)$ can be replaced by a kernel function $K(\mathbf{x}_i, \mathbf{x}_j)$ satisfying Mercer's theorem ([16]). In this way, the input space is implicitly mapped to some other high-dimensional feature space, where the data are better described from the hypersphere. Equation (22) reads then in the new feature space:

$$\begin{aligned} \Delta(\mathbf{z}) = K(\mathbf{z}, \mathbf{z}) - 2 \sum_i \alpha_i K(\mathbf{z}, \mathbf{x}_i) \\ + \sum_{i,j} \alpha_i \alpha_j K(\mathbf{x}_i, \mathbf{x}_j). \end{aligned} \tag{23}$$

A common choice for the kernel function is the Gaussian kernel, defined as:

$$K(\mathbf{x}_i, \mathbf{x}_j) = \exp\left(\frac{-\|\mathbf{x}_i - \mathbf{x}_j\|^2}{\sigma^2}\right), \tag{24}$$

where σ is a width parameter. This kernel is independent of the position of the dataset with respect to the origin, i.e. only the distance between objects matters. Objects are mapped to unit norm vectors, so that only the angles between them count ([13]). In the standard SVDD setting, objects are rejected and flagged as outliers when they lie outside the hypersphere ($\Delta > R^2$). Optimal selection of the model parameters (C and σ) is still an open issue in data description problems. In this article, the approach proposed by Tax in [40] using grid-search was taken.

2.3. Proposed methodology

A variation in the operating conditions of the machine affects the CI values (RMS and Kurtosis in the present case) through the variation of the measured response (1). Hence, CI values are correlated to the operating condition parameters. Studies on the correlation among different CI and with between CI and operating conditions are reported in [9]. There is evidence for strongly non-linear correlation. Ideally, such a correlation would change with mechanical degradation progressively affecting the measured response signal. Therefore, it is proposed to extend the idea described in [11] of fusing multiple CI in an AS (therein referred to as Health Indicator), keeping into account the non-linearities in the correlation between indicators induced from the underlying unknown operating variables. The idea behind the AS is then to exploit the correlation information in order to obtain better separation between the healthy state and the faulty state of a given component, under the assumption that given a sufficient amount of observations, vibration data will be acquired under similar conditions for a helicopter operating similar mission profiles. In order to hold the non-linearities in the CI correlation model, an SVDD for the healthy distribution is proposed instead of a Gaussian one. The metric for the AS was selected to be the distance of an observation from the center of the hyper-sphere in the kernel space, according to equation (23). The metric of the AS for the Gaussian model was computed as the squared Mahalanobis Distance ([41]) of an observation to the learnt Gaussian model, according to [11]. The algorithm involves a learning phase, in which models are trained using N_{train} observations, and an evaluation phase in which new observations are compared to the model and an AS obtained. The learning phase can be triggered from the operator after any relevant maintenance action, manually entered or automatically detected with methods such the one mentioned, e.g. in [11]. The issue of setting a threshold on the AS values in order to decide whether an observation is normal or not is not addressed in this work, since it involves several additional steps which are part of the overlying logic (see figure 1). Seemingly, N_{train} needs to be determined according to the maintenance policy and is considered given as a constraint in this work.

3. Results

3.1. Preliminary data characterization

Flight data have been recorded from two piezoelectric accelerometers mounted on the gearbox case of a H 135 helicopter. The monitoring system with which the considered helicopter was equipped recorded the output acceleration from seven sensors at different locations. Three of them are dedicated to monitoring the cabin vibration, one to the tail drive shaft, one to the tail gearbox and the latter two to the main gearbox. A sketch of the main gearbox is shown in figure 2. The two input drive shafts rotate at a speed of about 98.3Hz (≈5900rpm) and transmit power from the engines to the main gearbox. Shafts speed ranges from about 6.5Hz at the main hub shaft to 210Hz at the fan drive shaft at 100% nominal engine speed. The main gearbox accelerometers are located on the right and left side of the casing, in proximity of the input drive shafts and measure the radial acceleration with a sampling frequency of 7000Hz. For monitoring purposes, the system periodically acquires 2.85s of vibration data, corresponding to 20000 stored samples per acquisition per accelerometer. The system starts recording only when flight conditions are stable (contextual correction in figure 1), as to prevent from acquiring highly non-stationary vibration data (e.g. during start-up), this restricts the space of possible occurring operating conditions during a record. A first effect of the constraint is reducing the number of acquisitions in a given period, the second is that of imposing a first limitation to the CI values variability due to the different operating conditions. Additionally, due to memory constraints from the acquisition system, a maximum number of five files is stored during each flight session. Together with vibration, a magnetic pickup installed on the main rotor swash plate and one on the tail rotor store a synchronizing signal, allowing for the establishment of angle/time relationships used for resampling of the TSA signal. The mechanical complexity of the system and the flight environment results in multiple vibration sources, mainly consisting of main rotor and blades vibration, wind/structure interactions and other aerodynamic effects and vibration directly related to the rotating components, like unbalanced/misaligned shafts or meshing gears. The mixture of all these sources is transmitted through the structure to the accelerometers according to model (1), giving rise to a profuse spectrum in which characteristic frequencies are hardly identifiable. A typical measured spectrum in a fault-free condition is shown in figure 3. The peak of the response at about 2260Hz is the meshing frequency of the input drive gear and the intermediate shaft output pinion. Such a noisy spectrum justifies the introduction of signal processing techniques, based on a first-principle understanding of the effect that the developing damage has on the measured vibration signal (section 2.1.2). The data used for this analysis were acquired during almost 22 months of operating life of the helicopter (≈2130 Flight Hours). In this time frame, micro-pitting degradation occurred on the right input drive shaft's pinion. Ground truth is available from two inspections carried on after 1600 FH and 2130 FH. After the first inspection, the measured damaged area was about 16mm^2 and was judged safe for the operations of the gears. The damaged area at the time of the second inspection was about 34mm^2 and the asset was then replaced. The degradation is visible in the form of gray staining on the tooth surface (figure 4). The damage started developing between 1000 FH and the date of first assessment. However, no feedback on direct inspections of the component is available before the 1600 FH inspection.

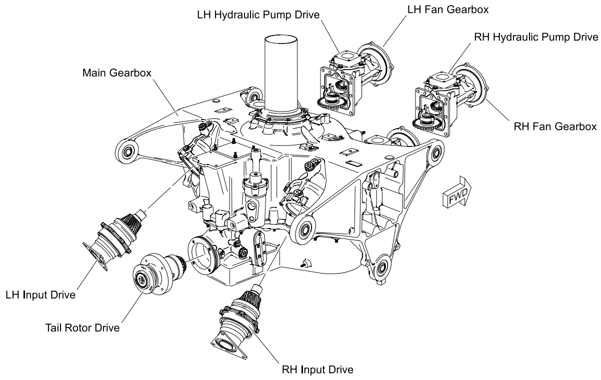

Figure 2: H 135 main gearbox.

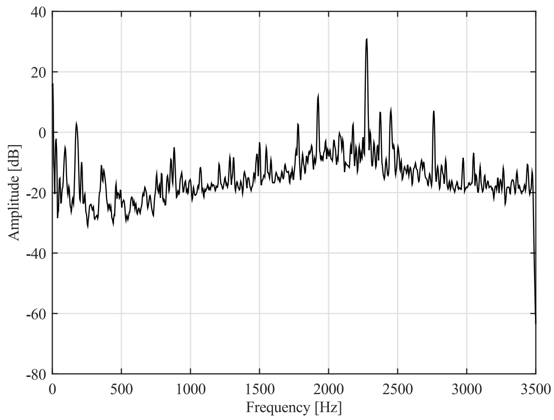

Figure 3: Spectrum of a 2.85s fault-free vibration signal recorded in flight by one of the monitoring system main gearbox accelerometer with a sampling frequency of 7000Hz (estimated using Hanning window and 16 non-overlapping averages).

3.2. Fault detection performance

For verification purposes, and with reference to the previously reported maintenance inspections, the flight data were divided in the following sequential blocks:

1. Healthy state (≈1000 FH);
2. Early degradation (unknown state) (≈600 FH);
3. Known degradation (faulty state) (≈530 FH).

The proposed methodology, based on AS generation through SVDD data fusion is assessed by comparing its performance in detecting the early degradation with respect to the univariate analysis of the CI proposed in section 2.1 and with respect to the method based on the Gaussian model proposed in [11]. First, the CI computed over the entire data history are presented. Next, the Gaussian and the proposed method are applied using $N_{train} = 80$ acquisitions for training and the remaining for evaluation of the AS. Since the goodness of the obtained multivariate model depends on some extent on the representativeness of the training set, the models were trained picking all the possible training sets from the healthy data. In this way, robustness to poor representative training sets is accounted for. Classification performance can be measured independently from threshold setting by introducing the receiving operating characteristic (ROC) curves. Such curves represent the fraction of target object accepted by the model (i.e. healthy observations classified as healthy) against the fraction of outliers accepted (i.e. faulty observations classified as healthy). The area under the ROC curve (AUC) gives a scalar measure of the achieved separability between states. Computing the classification performances requires the definition of a healthy and a faulty dataset. The healthy dataset was defined including the first 1000 FH, whereas four definitions are introduced for the faulty state: early stage degradation (from FH 1150); middle stage degradation (from FH 1300); advanced stage degradation (from FH 1450) and assessed degradation (from FH 1600). The models were evaluated in the four cases, which allows for comparing their efficiency in responding early to the fault development in terms of AUC, without introducing model-specific thresholds or novel key performance indexes. The CI extracted from the vibration data were computed as described in section 2.1. Figure 5 shows the values of the RMS and Kurtosis indicators computed from the shaft-synchronous signal. The dates in which damage was assessed are indicated with black vertical lines. Although there is a clear upward trend correlated with the degradation, the values are very scattered and present a complex distribution. A visualization of the CI distribution in the healthy state is shown in figure 6, where the quantiles of the CI distributions are plotted against the quantiles of the normal distribution. It can be seen that both the CI distributions do not match the Gaussian (dashed line in the figure). In figure 7, scatter plots of the CI centred in the feature space normalized by their mean are shown. The contours of example data descriptions obtained using the Gaussian model and the SVDD model are plotted for varying AS values. It is evident that the SVDD model produces a tighter description, which results in a better ability of discriminating between those data points belonging to the healthy distribution all the others not belonging to it. The ROC curves in the four degradation cases mentioned above are shown in figure 8. The curves for the multivariate models are obtained as mean ROC curves over all the possible 4680 ROC curves computed on training

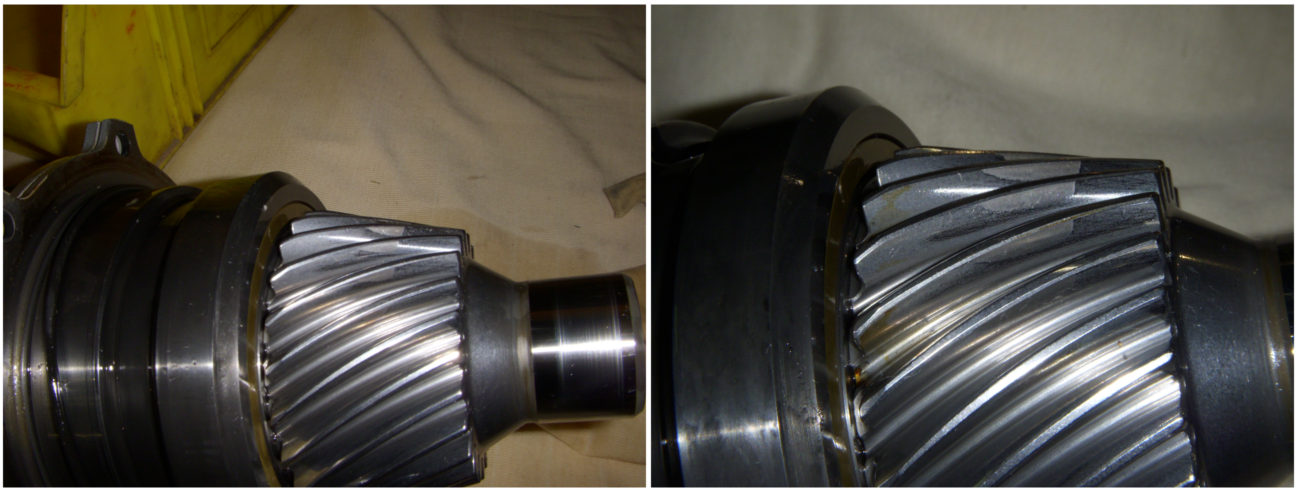

(a) **(b)**

Figure 4: Gray staining on the right input drive shaft's pinion. a) Component at the time of first inspection; b) component at the time of second inspection.

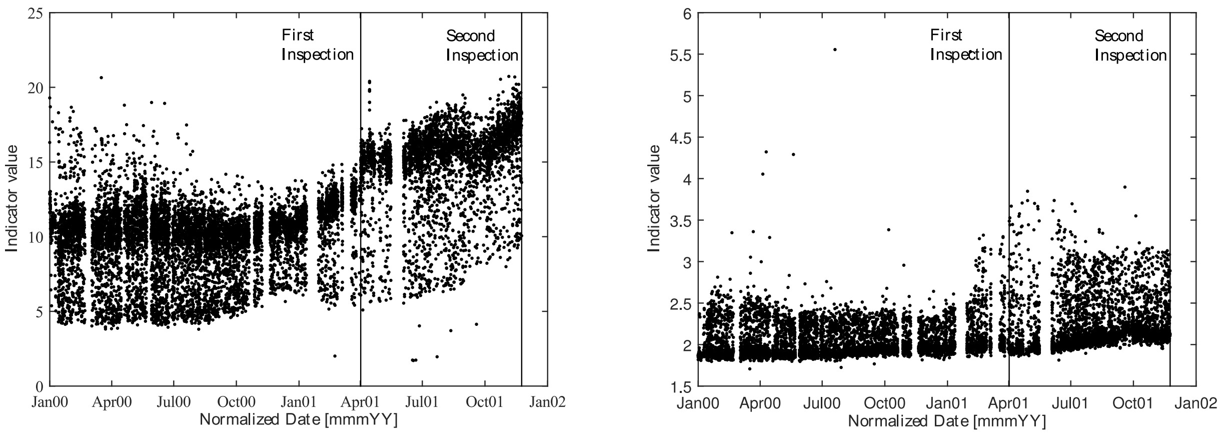

(a) **(b)**

Figure 5: Time history of the condition indicators (time axis is translated such that the first acquisition coincides with the reference date of 01 Jan 00). Black vertical lines: first inspection and second inspection. a) RMS CI; b) Kurtosis CI.

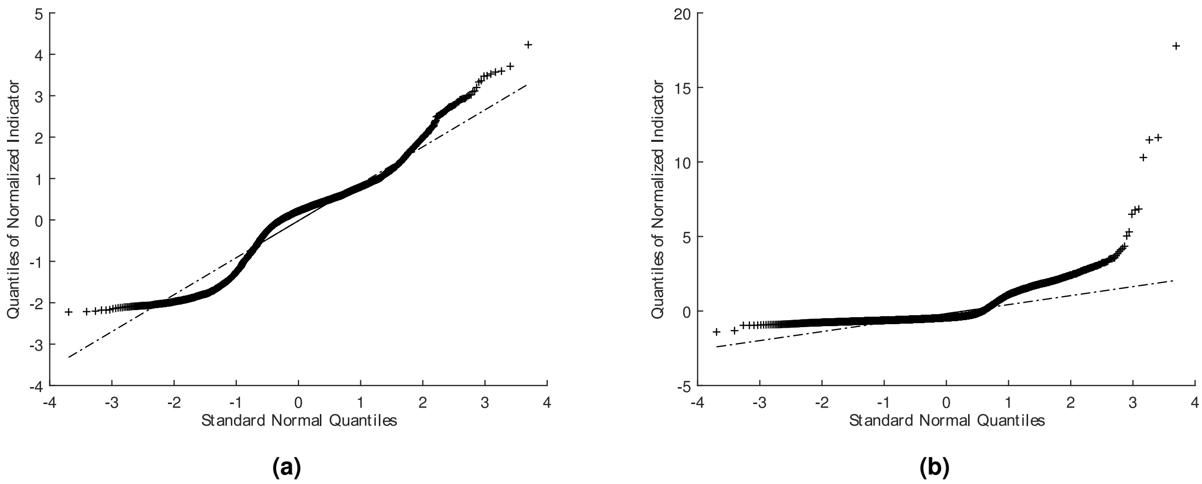

Figure 6: Normality test of each CI visualized through quantile-quantile plots. a) RMS CI; b) Kurtosis CI.

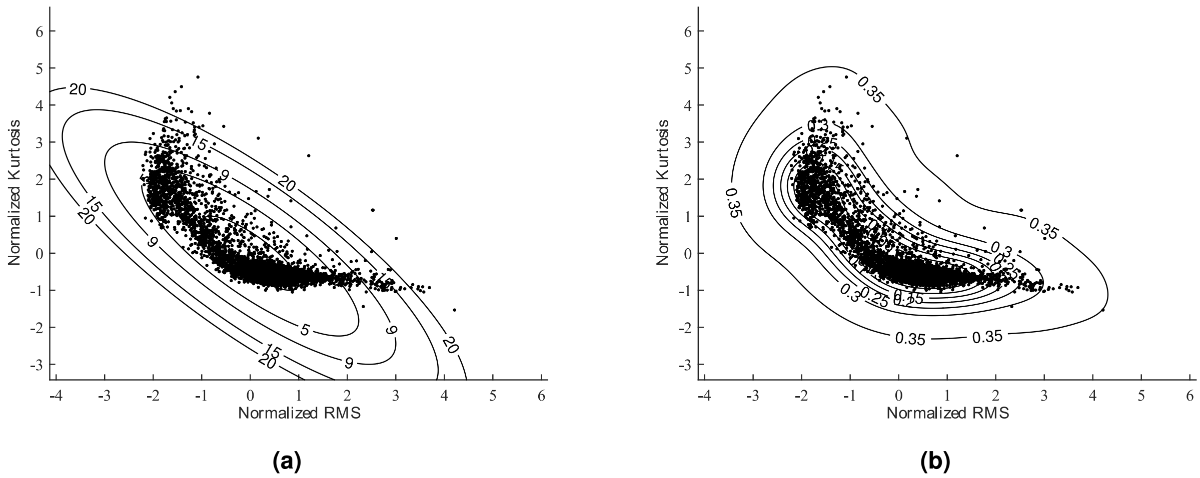

Figure 7: Scatter plots of the CI in the normalized feature space and contours representing varying AS. a) Gaussian model contours; b) SVDD model contours.

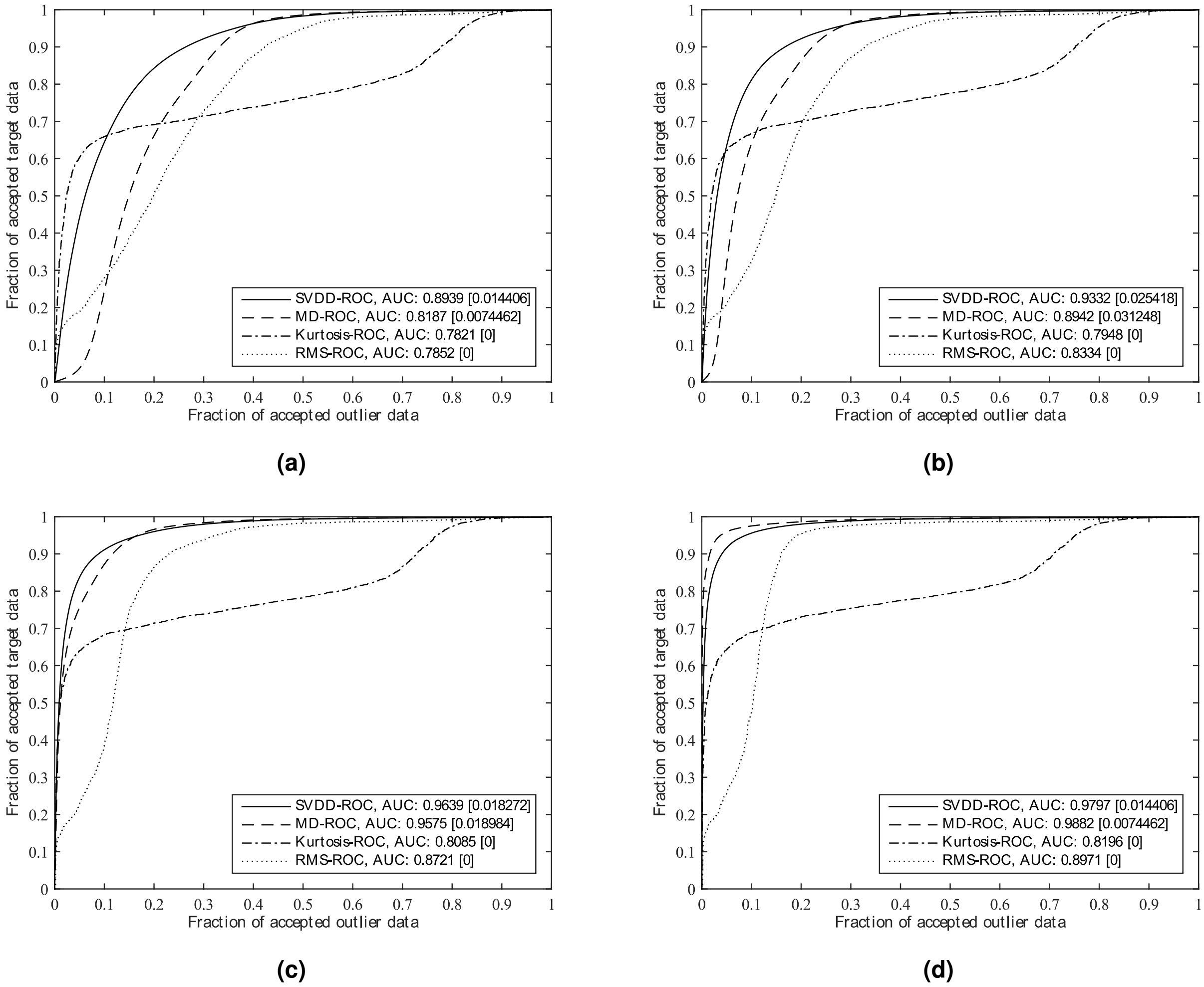

Figure 8: ROC curves. SVDD and Gaussian model average performance over 4680 training sets compared with univariate CI performance in the four degradation stages. a) Early stage degradation; b) middle stage degradation; c) advanced stage degradation and d) minimum assessed micro-pitting of 16mm^2

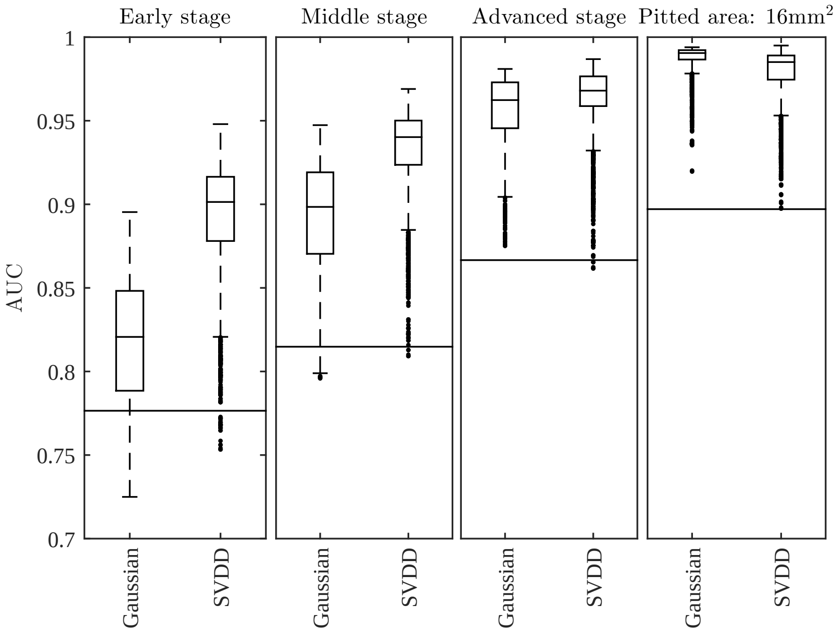

Figure 9: Boxplot of AUC values obtained in the four degradation cases for the Gaussian and SVDD models over the 4680 evaluations, compared to the AUC of the best performing CI (black lines in the plot).

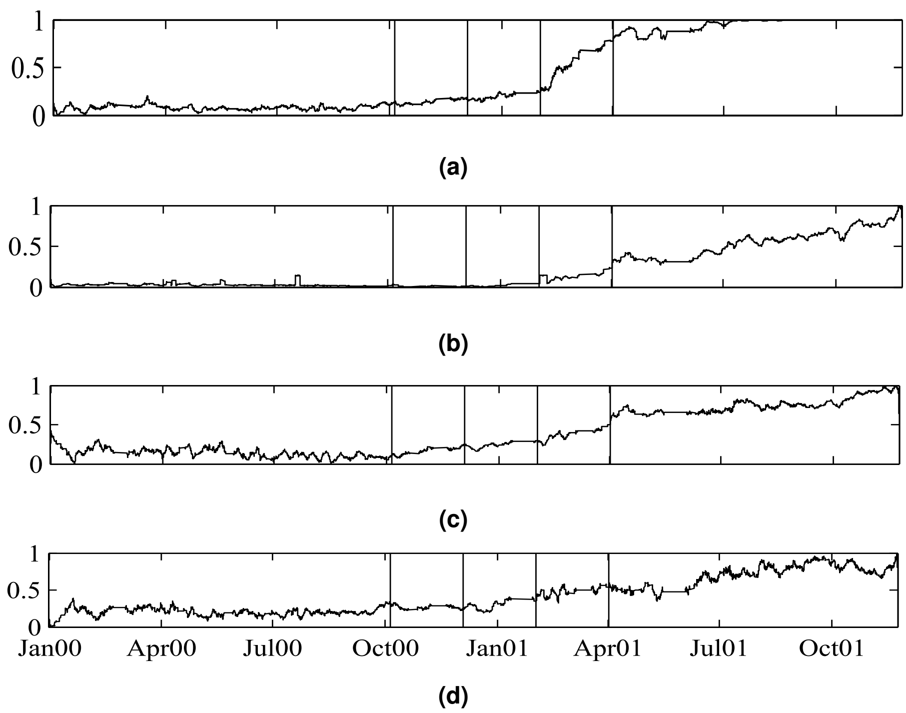

Figure 10: Trend values of the AS and the CI computed using a moving average filter with a length of 100 acquisitions (time axis is translated such that the first acquisition coincides with the reference date of 01 Jan 00). a) SVDD AS; b) Gaussian AS; c) RMS; d) Kurtosis.

sets obtained drawing a sequence of N_{train} acquisitions from the healthy distribution. The mean AUC, computed from the mean ROC curve, is reported in the legend along with the AUC values standard deviation in squared brackets. The indicators (both from the multivariate and from the univariate models) gain a better discriminating ability with the damage progression. This is not surprising, since the CI are designed for being correlated with fault evolution and hence their value increase with the defect growth. However, both the multivariate indicators performs better in general. Moreover, they offer the advantage of resuming the information from multiple CI in one single AS, thus enabling simpler decision. For early and middle stage damage (figures 8a and 8b), Kurtosis indicator performs better than all the other indicators in the low target acceptance rate region. This means that for threshold settings generating very high false alarm rates it has higher probability of detecting anomalous observations. RMS performs worst at almost every acceptance rate. The AS computed from SVDD model is the one granting highest probabilities of detection at a given probability of false alarm in the early, middle and advanced degradation stages, whereas for more several degradation (first inspection onward), the Gaussian model performs slightly better on average, since the healthy and faulty distributions becomes very well separated in the features space. Except for the last stage, the SVDD model is more robust to the variability of the training set with respect to the Gaussian model, as observed from the standard deviation values. In order to better visualize the influence of different training sets, a boxplot of the AUC values in the four stages is shown in figure 9. Training sets which are more representatives of the real multivariate distribution of the indicators leads in general to higher AUC scores for the multivariate models. The horizontal black lines in the plot represent the AUC computed for the best-performing univariate CI. In general, the SVDD model results in higher AUC than the univariate models for almost all the possible training sets, yielding an AUC relatively close to that of the univariate CI in the few cases in which they perform better. The Gaussian model suffers more from the training set representativeness in the first three considered degradation stages. However, in the majority of the cases it yields better performance than the univariate indicators, outperforming also the SVDD model when considering the severe degradation case. Tables 1 to 4 summarize the comparison between SVDD AS and Gaussian AS for the four considered degradation cases, by the mean of three parameters. The first one is the average AUC gain (AAG), defined as the difference between the mean AUC value obtained over all the training sets and the best AUC value from the univariate CI. The second parameter is the failure rate (FR), defined as the count of the cases in which the multivariate model performed worst than the best univariate CI divided by the total number of cases (4680). The third introduced parameter is the worst AUC loss (WAL), defined as the difference between the best AUC from the univariate CI and the worst case AUC valued obtained for the AS. From the tables, the AS from SVDD model outperform both the AS from Gaussian model and the univariate CI for early detection. Once the fault condition is sufficiently developed, it seems that the Gaussian model performs slightly better with respect to the SVDD, owing to the increased topological separation between the cluster of the anomalous points and that of the reference distribution in the CI space. However, both the multivariate models consistently outperform the traditional univariate CI analysis. These results translate into a clearer ability of the AS of reacting to the faults with respect to the CI, as shown in figure 10, where the AS and CI trends are compared. Trend analysis of the CI is a common practice in the industry. Clearly considering the trend over more acquisitions helps to average out the scattering of the CI. Nevertheless, it comes at a price, since the need for more acquisitions for making a decision translates in reduced reaction time. Having indicators which are able of better separating faulty states from the healthy ones is therefore preferable, since using the same number of points, increased confidence in the decision can be obtained, whatever the decision policy is. In figure 10, trends are obtained using a moving average filter with a length of 100 acquisitions. The black vertical lines indicate the beginning of each of the four defined sequential degradation stages. It is observed that the AS from the SVDD model is reacting quicker to the fault initiation, resulting in improved fault detection ability.

Table 1: Comparison of AS and CI performance, early stage degradation

Parameter	Gaussian model	SVDD model
AAG	0.0422	**0.1174**
FR	0.1558	**0.0064**
WAL	0.0515	**0.0232**

Table 2: Comparison of AS and CI performance, middle stage degradation

Parameter	Gaussian model	SVDD model
AAG	0.0794	**0.1184**
FR	0.0058	**0.0011**
WAL	0.019	**0.0056**

Table 3: Comparison of AS and CI performance, advanced stage degradation

Parameter	Gaussian model	SVDD model
AAG	0.0909	**0.0973**
FR	**0**	0.0011
WAL	**-**	0.005

Table 4: Comparison of AS and CI performance, minimum assessed micro-pitted area of $16mm^2$

Parameter	Gaussian model	SVDD model
AAG	**0.1216**	0.1131
FR	0	0
WAL	-	-

4. Conclusion

As a main result, this work showed the possibility of obtaining improved information from Health and Usage Monitoring Systems vibration data by fusing traditional CI into single AS using data description models. Such an improvement is achieved by considering the variability induced by the operating conditions of the helicopter on the CI values implicitly inside the AS models, in the form of a correlation between multiple CI through latent variables. The models are learnt from the acquired data during a learning phase of the algorithm. Therefore, a set of reference values are needed before the monitoring can be effectively enabled. Remarkably, since operating conditions are treated as latent variables, there is no need for direct measurements of the flight parameters. In order to address the limits of the original proposal based on a Gaussian model, an SVDD model was introduced. The method allowed to obtain an AS which improved the detection of early stage degradation with respect to the AS obtained from the Gaussian model and with respect to traditional univariate CI. Moreover, only few training acquisitions were sufficient for learning a proper data description. The choice of the model parameters was automatized, yielding good results for the considered case. There is no warranty, in any case, that optimizing on an artificially-generated outlier (faulty) data will result in good performance on the real outlier (faulty) data distribution. The method assessment was performed on comprehensive real operating vibration data. It was shown that although the multivariate models depend on some extent on the training set representativeness of the true distribution, reasonably robust performance improvements could be obtained over the univariate CI. However, no general indication can be given on the minimum number of the training acquisitions necessary for an accurate description of a set of CI, which greatly depends on the characteristics of the distribution. Future research for HUMS improvement should be addressed to gaining a major understanding of the modality through which vibration response signals are affected from the various sources encountered in real operations environment.

References

[1] Anthony RS Bramwell, David Balmford and George Done. *Bramwell's helicopter dynamics*. Butterworth-Heinemann, 2001.

[2] U.S. Army. *ADS-79C-HDBK, Aeronautical Design Standard: Handbook for Condition Based Maintenance Systems for US Army Aircraft Systems*. 2012.

[3] Abdel Bayoumi et al. "Conditioned-Based Maintenance at USC-Part I: Integration of Maintenance Management Systems and Health Monitoring Systems through Historical Data Investigation". In: *Proceedings of the AHS International Specialists Meeting on Condition Based Maintenance, Huntsville, AL*. 2008.

[4] Brian D Larder, Mark W Davis and CT Stratford. "HUMS Condition Based Maintenance Credit Validation". In: *American Helicopter Society 63rd Annual Forum*. 2007.

[5] Johan Wiig. "Optimization of fault diagnosis in helicopter health and usage monitoring systems". PhD thesis. Aix-en-Provence, ENSAM, 2006.

[6] Venkat Venkatasubramanian et al. "A review of process fault detection and diagnosis: Part I: Quantitative model-based methods". In: *Computers & chemical engineering* 27.3 (2003), pp. 293–311.

[7] Paula J Dempsey, David G Lewicki and Dy D Le. "Investigation of current methods to identify helicopter gear health". In: *Aerospace Conference, 2007 IEEE*. IEEE. 2007, pp. 1–13.

[8] Akm Anwarul Islam et al. *Characterization and comparison of vibration transfer paths in a helicopter gearbox and a fixture mounted gearbox*. Tech. rep. TM-216586. NASA, 2014.

[9] Marianne Mosher, Edward M Huff and Eric Barszcz. "Analysis of in-flight measurements from helicopter transmissions". In: *American Heliopter Society 60th Annual Forum, Baltimore*. 2004.

[10] *Intelligent management of helicopter vibration health monitoring data: Based on a report prepared for the CAA by GE Aviation Systems Limited*. Vol. 2011/01. CAA paper. Norwich: Published by TSO on behalf of UK Civil Aviation Authority, 2012. ISBN: 9780117924031.

[11] S Bendisch and J Mouterde. "New methodologies to improve health and usage monitoring system (HUMS) performance using anomaly detection applied on helicopter vibration data". In: *39th European Rotorcraft Forum, Moscow*. 2013.

[12] Georg Wurzel. "Development of a Condition-Based Maintenance Concept for Helicopter Drive Systems". PhD thesis. Vienna University of Technology, 2011.

[13] David MJ Tax and Robert PW Duin. “Support vector data description”. In: *Machine learning* 54.1 (2004), pp. 45–66.
[14] Zhiqiang Ge, Furong Gao and Zhihuan Song. “Batch process monitoring based on support vector data description method”. In: *Journal of Process Control* 21.6 (2011), pp. 949–959.
[15] Sang-Woong Lee, Jooyoung Park and Seong-Whan Lee. “Low resolution face recognition based on support vector data description”. In: *Pattern Recognition* 39.9 (2006), pp. 1809–1812.
[16] David MJ Tax and Robert PW Duin. “Support vector domain description”. In: *Pattern recognition letters* 20.11 (1999), pp. 1191–1199.
[17] Carolina Sanchez-Hernandez, Doreen S Boyd and Giles M Foody. “Mapping specific habitats from remotely sensed imagery: support vector machine and support vector data description based classification of coastal saltmarsh habitats”. In: *Ecological informatics* 2.2 (2007), pp. 83–88.
[18] D Tax, Alexander Ypma and R Duin. “Support vector data description applied to machine vibration analysis”. In: *Proc. 5th Annual Conference of the Advanced School for Computing and Imaging (Heijen, NL)*. Citeseer. 1999, pp. 398–405.
[19] Yuna Pan, Jin Chen and Lei Guo. “Robust bearing performance degradation assessment method based on improved wavelet packet–support vector data description”. In: *Mechanical Systems and Signal Processing* 23.3 (2009), pp. 669–681.
[20] Alexander Ypma, David MJ Tax and Robert PW Duin. “Robust machine fault detection with independent component analysis and support vector data description”. In: *Neural Networks for Signal Processing IX, 1999. Proceedings of the 1999 IEEE Signal Processing Society Workshop.* IEEE. 1999, pp. 67–76.
[21] Dong Wang et al. “Support vector data description for fusion of multiple health indicators for enhancing gearbox fault diagnosis and prognosis”. In: *Measurement Science and Technology* 22.2 (2010), p. 025102.
[22] WJ Wang and PD McFadden. “Early detection of gear failure by vibration analysis i. calculation of the time-frequency distribution”. In: *Mechanical Systems and Signal Processing* 7.3 (1993), pp. 193–203.
[23] B David Forrester. “Advanced vibration analysis techniques for fault detection and diagnosis in geared transmission systems”. PhD thesis. 1996.
[24] F Combet and L Gelman. “Optimal filtering of gear signals for early damage detection based on the spectral kurtosis”. In: *Mechanical Systems and Signal Processing* 23.3 (2009), pp. 652–668.
[25] G Dalpiaz, A Rivola and R Rubini. “Effectiveness and sensitivity of vibration processing techniques for local fault detection in gears”. In: *Mechanical Systems and Signal Processing* 14.3 (2000), pp. 387–412.
[26] CJ Stander, PS Heyns and W Schoombie. “Using vibration monitoring for local fault detection on gears operating under fluctuating load conditions”. In: *Mechanical Systems and Signal Processing* 16.6 (2002), pp. 1005–1024.
[27] N Baydar and Andrew Ball. “Detection of gear failures via vibration and acoustic signals using wavelet transform”. In: *Mechanical Systems and Signal Processing* 17.4 (2003), pp. 787–804.
[28] Jérôme Antoni. “The spectral kurtosis: a useful tool for characterising non-stationary signals”. In: *Mechanical Systems and Signal Processing* 20.2 (2006), pp. 282–307.
[29] Jérôme Antoni and RB Randall. “The spectral kurtosis: application to the vibratory surveillance and diagnostics of rotating machines”. In: *Mechanical Systems and Signal Processing* 20.2 (2006), pp. 308–331.
[30] Alexander Ypma. “Learning methods for machine vibration analysis and health monitoring”. PhD thesis. 2001.
[31] Victor Girondin et al. “Bearings fault detection in helicopters using frequency readjustment and cyclostationary analysis”. In: *Mechanical Systems and Signal Processing* 38.2 (2013), pp. 499–514.
[32] WJ Wang and PD McFadden. “Decomposition of gear motion signals and its application to gearbox diagnostics”. In: *Journal of Vibration and Acoustics* 117.3A (1995), pp. 363–369.
[33] PD McFadden. “A revised model for the extraction of periodic waveforms by time domain averaging”. In: *Mechanical Systems and Signal Processing* 1.1 (1987), pp. 83–95.
[34] S Braun. “The synchronous (time domain) average revisited”. In: *Mechanical Systems and Signal Processing* 25.4 (2011), pp. 1087–1102.
[35] David Siegel, Jay Lee and Paula Dempsey. “Investigation and Evaluation of Condition Indicators, Variable Selection, and Health Indication Methods and Algorithms For Rotorcraft Gear Components”. In: *MFPT 2014 Conference, Virginia Beach, VA*. 2014.
[36] Vladimir Vapnik, Steven E Golowich and Alex Smola. “Support vector method for function approximation, regression estimation, and signal processing”. In: *Advances in neural information processing systems 9*. Citeseer. 1996.
[37] Bernhard Scholkopf. “Support Vector Machines: A Practical Consequence of Learning Theory”. In: *IEEE Intelligent systems* 13 (1998).
[38] Bernhard Schölkopf et al. “Estimating the support of a high-dimensional distribution”. In: *Neural computation* 13.7 (2001), pp. 1443–1471.
[39] Wei-Cheng Chang, Ching-Pei Lee and Chih-Jen Lin. *A revisit to support vector data description (SVDD)*. Tech. rep. Citeseer, 2013.
[40] David MJ Tax and Robert PW Duin. “Uniform object generation for optimizing one-class classifiers”. In: *The Journal of Machine Learning Research* 2 (2002), pp. 155–173.
[41] Prasanta Chandra Mahalanobis. “On the generalized distance in statistics”. In: *Proceedings of the National Institute of Sciences (Calcutta)* 2 (1936), pp. 49–55.